

DISTRIBUTED RECONSTRUCTION OF TIME-VARYING SPATIAL FIELDS BASED ON CONSENSUS PROPAGATION

Valentin Schwarz and Gerald Matz

Institute of Communications and Radio-Frequency Engineering, Vienna University of Technology
Gusshausstrasse 25/389, A-1040 Vienna, Austria; email: {vschwarz,gmatz}@nt.tuwien.ac.at

ABSTRACT

This work deals with the distributed measurement and reconstruction of time-varying spatial fields using wireless sensor networks (WSN). We use basis functions to formulate a low-dimensional subspace model for the field and estimate the field coefficients using a suitably modified version of consensus propagation (CP), which is a distributed asynchronous averaging algorithm with favorable convergence. Simulation results confirm the excellent performance of the proposed method in static and dynamic environments.

Index Terms— Consensus propagation, wireless sensor networks, field reconstruction, distributed inference

1. INTRODUCTION

In this paper, we propose to use consensus propagation (CP) [1] for field reconstruction in wireless sensor networks (WSN). CP is one of various approaches that have been introduced for computing averages in a distributed manner [2, 3]. CP views averaging as a convex optimization problem that is solved in a fully distributed manner via Gaussian belief propagation (message passing). The discussion of the convergence of Gaussian belief propagation in [4, 5] thus also applies to CP. A more specific analysis of CP is presented in [1, 6].

The WSN considered consists of I sensors that take measurements z_i , $i = 1, \dots, I$, and are capable to communicate with each other. The topology of the WSN is modeled by an undirected connected (communication) graph $\mathcal{G} = (\mathcal{V}, \mathcal{E})$, where the vertex set \mathcal{V} equals the set of sensors and the edge set \mathcal{E} contains the bidirectional communication links. We assume that each sensor knows its neighbors (i.e., the sensors it can directly communicate with) and its position.

With CP, the arithmetic mean $\bar{z} = \frac{1}{I} \sum_{i=1}^I z_i$ of the sensor measurements is calculated in an iterative manner. During iteration n , node i sends the following messages to node j :

$$K_{i \rightarrow j}^{(n)} = \frac{1 + \sum_{v \in \mathcal{N}(i) \setminus j} K_{v \rightarrow i}^{(n-1)}}{1 + \frac{1}{\beta} \left(1 + \sum_{v \in \mathcal{N}(i) \setminus j} K_{v \rightarrow i}^{(n-1)} \right)}, \quad (1)$$

$$\mu_{i \rightarrow j}^{(n)} = \frac{z_i + \sum_{v \in \mathcal{N}(i) \setminus j} \mu_{v \rightarrow i}^{(n-1)} K_{v \rightarrow i}^{(n-1)}}{1 + \sum_{v \in \mathcal{N}(i) \setminus j} K_{v \rightarrow i}^{(n-1)}}. \quad (2)$$

Here, $\mathcal{N}(i)$ denotes the set of neighbors of node i and β is a positive real-valued parameter. Using these messages, each node computes a

local estimate of \bar{z} during the n th iteration according to

$$\hat{z}_i^{(n)} = \frac{z_i + \sum_{v \in \mathcal{N}(i)} \mu_{v \rightarrow i}^{(n-1)} K_{v \rightarrow i}^{(n-1)}}{1 + \sum_{v \in \mathcal{N}(i)} K_{v \rightarrow i}^{(n-1)}}.$$

In [1, 6] it is shown that $\lim_{n \rightarrow \infty} \hat{z}_i^{(n)} = \bar{z}$ for all i as β goes to infinity.

We emphasize that the message updates in (1), (2) can be performed in a completely asynchronous manner.

In [7], we have proposed an equivalent broadcast version of CP that reduces the number of messages sent per iteration from $2|\mathcal{E}|$ to $|\mathcal{V}|$, resulting in a corresponding reduction of the transmit power. A similar broadcasting approach for general Gaussian belief propagation has been independently introduced in [8].

In this paper, we present a modification of CP that applies to the problem of distributed reconstruction of time-varying spatial fields. Our approach builds on a subspace model for the spatial field in which the coefficients are potentially time-varying (Section 2). Field reconstruction is accomplished by suitably adapting CP such that a distributed implementation of the least-squares (LS) estimator of the field coefficients is obtained (Section 3). Simulation results illustrate the performance of the proposed scheme in static and dynamic environments (Section 4).

2. FIELD MODEL AND MEASUREMENT

Subspace Model. Let us consider a real-valued time-varying spatial field $f(\mathbf{x}; t)$ defined in a prescribed region \mathcal{A} (\mathbf{x} denotes the spatial coordinates and t denotes time). Motivated by the smooth nature of most physical fields, we model their limited number of degrees of freedom via a subspace, i.e., we assume that the field belongs to an L -dimensional subspace $\text{span}\{u_1(\mathbf{x}), \dots, u_L(\mathbf{x})\}$ spanned linearly independent real-valued basis functions $u_l(\mathbf{x})$, $l = 1, \dots, L$. More specifically,

$$f(\mathbf{x}; t) = \sum_{l=1}^L c_l(t) u_l(\mathbf{x}), \quad (3)$$

where $c_l(t)$ denotes the time-varying field coefficients. The choice of the basis functions depends on the specific application. With regard to performance, it is desirable that the basis functions are chosen according to the following guidelines:

- the basis should be matched to the field under consideration in order to keep modeling errors as small as possible;
- the set $\{u_1(\mathbf{x}), \dots, u_L(\mathbf{x})\}$ should be orthonormal, i.e., $\int u_k(\mathbf{x}) u_l(\mathbf{x}) d\mathbf{x} = \delta_{kl}$ for all $k, l \in \{1, \dots, L\}$, so that the LS estimator matrix can be suitably approximated (see Section 3);

Funded by WWTF Grant ICT-044 and FWF Grant N10606.

- the basis functions should be robust to localization errors in the sense that $u_l(\mathbf{x} + \delta) \approx u_l(\mathbf{x})$ for a small position error δ .

A simple way for generating a spatial basis from a one-dimensional basis $\tilde{u}_k(x)$ results from the assumption of spatial separability, which in the 2-D case ($\mathbf{x} = (x, y)$) reads

$$u_l(x, y) = \tilde{u}_{k_1(l)}(x) \tilde{u}_{k_2(l)}(y). \quad (4)$$

At any time instant t the field is completely specified by the coefficients $c_l(t)$. Hence, reconstructing $f(\mathbf{x}; t)$ from sensor measurements amounts to determining $c_l(t)$, $l = 1, \dots, L$.

Sensor Measurements. The i th node in the WSN is located at position $\mathbf{x}_i \in \mathcal{A}$ and correspondingly measures the field sample

$$y_i[m] = f(\mathbf{x}_i; mT) + w_i[m], \quad (5)$$

where T denotes the temporal sampling period. Here, $w_i[m]$ subsumes the effects of modeling error, measurement noise, and quantization noise. Note that we assume synchronous temporal sampling for simplicity but we do not impose any model on the temporal dynamics of the field. For convenience, we arrange all sensor measurements into the length- I vector

$$\mathbf{y}[m] = (y_1[m] \ y_2[m] \ \dots \ y_I[m])^T.$$

With the definitions of the length- L vectors

$$\mathbf{u}_i = (u_1(\mathbf{x}_i) \ u_2(\mathbf{x}_i) \ \dots \ u_L(\mathbf{x}_i))^T, \quad (6)$$

$$\mathbf{c}[m] = (c_1(mT) \ c_2(mT) \ \dots \ c_L(mT))^T,$$

and the length- I vector $\mathbf{w}[m] = (w_1[m] \ w_2[m] \ \dots \ w_I[m])^T$, (3) and (5) can be combined and rewritten as

$$\mathbf{y}[m] = \mathbf{U}\mathbf{c}[m] + \mathbf{w}[m]. \quad (7)$$

Here, the $I \times L$ subspace matrix \mathbf{U} is given by $\mathbf{U} = (\mathbf{u}_1 \ \mathbf{u}_2 \ \dots \ \mathbf{u}_I)^T$.

3. DISTRIBUTED FIELD RECONSTRUCTION

LS Approach. In a centralized setup where the subspace basis and all sensor positions \mathbf{x}_i and measurements $y_i[m]$ are known to a single computation unit, the field coefficients can be estimated from (7) using an LS approach according to

$$\begin{aligned} \hat{\mathbf{c}}[m] &= \arg \min_{\mathbf{c}} \|\mathbf{y}[m] - \mathbf{U}\mathbf{c}\|^2 \\ &= (\mathbf{U}^T \mathbf{U})^{-1} \mathbf{U}^T \mathbf{y}[m] = \mathbf{U}^\# \mathbf{y}[m]. \end{aligned} \quad (8)$$

Here, $\mathbf{U}^\# = (\mathbf{U}^T \mathbf{U})^{-1} \mathbf{U}^T$ denotes the pseudo-inverse of \mathbf{U} . Our aim in the following will be to use CP to develop a distributed algorithm for computing $\hat{\mathbf{c}}[m]$. We impose the constraint that each sensor is required to know only its own position and measurement. We first show how to modify CP so that it can solve the LS problem in (8) under the unrealistic assumption that all sensors know the size I of the WSN and that sensor i knows exactly the i th column of $\mathbf{U}^\#$, denoted $\mathbf{u}_i^\#$, which has length L . Subsequently, we propose two approaches to approximating $\mathbf{u}_i^\#$ which simultaneously obviate the requirement of knowing I at each sensor.

CP-based Distributed Implementation. We first rewrite the LS solution (8) in a componentwise manner:

$$\hat{\mathbf{c}}[m] = \sum_{i=1}^I \mathbf{u}_i^\# y_i[m] = \frac{1}{I} \sum_{i=1}^I \mathbf{z}_i[m],$$

where we defined $\mathbf{z}_i[m] = \mathbf{u}_i^\# y_i[m] I$. Clearly, if sensor i knows I and $\mathbf{u}_i^\#$, computation of $\hat{\mathbf{c}}[m]$ is identical to computing the arithmetic mean of (all elements of) $\mathbf{z}_i[m]$ with respect to i . The latter task is exactly what CP has been designed for. Therefore, we can use the iterative message passing protocol of CP to obtain more and more refined estimates of $\hat{\mathbf{c}}[m]$. Since $\hat{\mathbf{c}}[m]$ has length L , we need L instances of CP which in principle could operate independently. However, we prefer to run those CP instances in parallel which amounts to exchanging vector messages. Since the ‘‘cardinality messages’’ $K_{i \rightarrow j}^{(n)}$ do not depend on the actual measurements (cf. (1)), they do not require any modification. The vectorized version of the μ -messages then reads

$$\boldsymbol{\mu}_{i \rightarrow j}^{(n)} = \frac{\mathbf{u}_i^\# y_i[m] I + \sum_{v \in \mathcal{N}(i) \setminus j} \boldsymbol{\mu}_{v \rightarrow i}^{(n-1)} K_{v \rightarrow i}^{(n-1)}}{1 + \sum_{v \in \mathcal{N}(i) \setminus j} K_{v \rightarrow i}^{(n-1)}} \quad (9)$$

where $m = \lfloor \frac{n}{N} \rfloor$ and L denotes the number of CP iterations per sampling period. The approximation of $\hat{\mathbf{c}}[m]$ computed by node i equals

$$\hat{\mathbf{c}}_i[m] = \frac{\mathbf{u}_i^\# y_i[m] I + \sum_{v \in \mathcal{N}(i)} \boldsymbol{\mu}_{v \rightarrow i}^{(n-1)} K_{v \rightarrow i}^{(n-1)}}{1 + \sum_{v \in \mathcal{N}(i)} K_{v \rightarrow i}^{(n-1)}}, \quad (10)$$

with $n = (m+1)N - 1$ (cf. [7]).

As we increase the number of CP iterations between successive sampling instances, the convergence properties of CP ensure that for $\beta \rightarrow \infty$ we have $\lim_{N \rightarrow \infty} \hat{\mathbf{c}}_i[m] = \hat{\mathbf{c}}[m]$ for all i , and thus each sensor can reconstruct the entire field. However, performing a large number of CP iterations within each sampling period may be undesirable since this requires repeated message transmission and hence consumes a rather large amount of energy. This may be acceptable in (quasi-)static scenarios where the field $f(\mathbf{x}; t)$ is (almost) independent of time and the sampling period T thus can be sufficiently large. For scenarios with stronger temporal dynamics and shorter sampling period, a more energy-efficient approach is to perform only a few iterations of CP per sampling period. Here, a rather small value for the ‘‘attenuation’’ parameter β should be used in order to reduce the response time of CP. We specifically favor the extreme case of only one iteration ($N = 1$) where $n = m$. In this case, each CP iteration involves a new sensor measurement and hence the convergence results developed for ordinary (static) CP do not apply. Nonetheless, our simulation results indicate that this approach is capable of accurately tracking the time-varying field provided its rate of change is not too large. Due to the response time inherent to CP, the field coefficient estimates are obtained with a certain delay that can be compensated for by using a linear prediction filter at each sensor (see [7]). The calculation of $\hat{\mathbf{c}}_i[m]$ according to (10) implicitly involves past measurements and thus behaves similarly as as LS estimator with exponential forgetting.

A drawback for the practical implementation of the field reconstruction protocol described above is the assumption that each sensor knows the number of sensors I and the i th column of $\mathbf{U}^\#$. Since $\mathbf{u}_i^\# = (\mathbf{U}^T \mathbf{U})^{-1} \mathbf{u}_i$, knowing $\mathbf{u}_i^\#$ exactly requires knowledge of all sensor positions $\{\mathbf{x}_i\}$ in order to be able to compute the elements of $\mathbf{U}^T \mathbf{U}$ via the inner products $[\mathbf{U}^T \mathbf{U}]_{k,l} = \sum_{i=1}^I u_k(\mathbf{x}_i) u_l(\mathbf{x}_i)$. Even though there are distributed algorithms for sensor localization (e.g. [9]), in many applications knowing all sensor positions at each

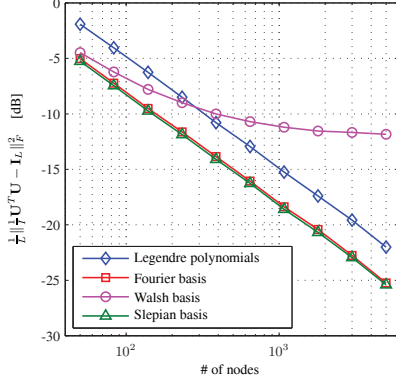


Fig. 1. Accuracy of orthogonal approximation versus number of sensors for different bases.

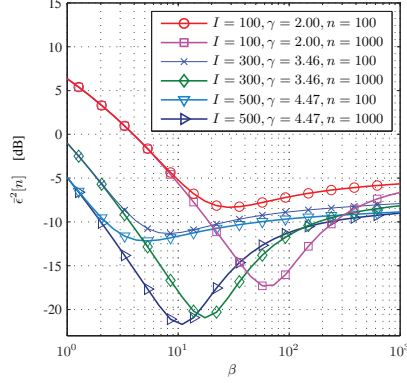
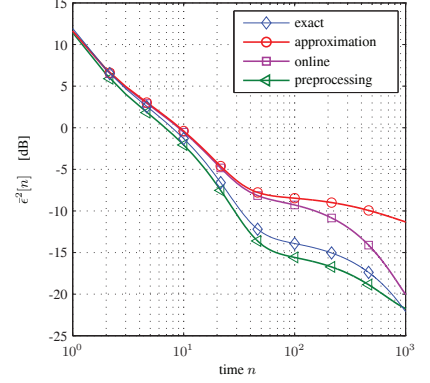


Fig. 2. Static field reconstruction performance: MSE versus β for various WSN scenarios (left), and MSE versus number of iterations for different algorithm variants (right).



node may be unrealistic or undesirable. Thus we next propose two approaches to obtain approximate knowledge of $\mathbf{u}_i^\#$ which implicitly also compensate for the factor I in the CP updates (9) and (10).

Orthogonal Approximation. The first approach builds on orthonormal basis functions $\{u_l(\mathbf{x})\}$. If the basis functions are band-limited and the sensors are placed on a sufficiently dense uniform lattice such that the Nyquist criterion is satisfied, the orthogonality is inherited by the sampled basis functions, i.e., $\sum_{i=1}^I u_k(\mathbf{x}_i) u_l(\mathbf{x}_i) = I \delta_{kl}$. The idea now is to assume that such orthogonality relations hold approximately true for arbitrary sensor placements, i.e.,

$$\mathbf{U}^T \mathbf{U} \approx I \mathbf{I}_L, \quad (11)$$

where \mathbf{I}_L denotes the $L \times L$ identity matrix. The accuracy of this approximation improves with increasing number of sensors (see Section 4). The approximation (11) implies $\mathbf{u}_i^\# = (\mathbf{U}^T \mathbf{U})^{-1} \mathbf{u}_i \approx \frac{1}{I} \mathbf{u}_i$ and hence further $\mathbf{z}_i[m] = \mathbf{u}_i^\# y_i[m] I \approx \mathbf{u}_i y_i[m]$. This approximation can be directly used in (9) and (10) to obtain CP iterations in which each sensor only needs to know its own position to determine \mathbf{u}_i according to (6).

CP-based Computation of the Gramian. For WSN with few or irregularly placed sensors, the approximation (11) may be too inaccurate. For such scenarios, we observe that the elements of the scaled Gramian $\mathbf{G} = \frac{1}{I} \mathbf{U}^T \mathbf{U}$ equal

$$[\mathbf{G}]_{k,l} = \frac{1}{I} \sum_{i=1}^I u_k(\mathbf{x}_i) u_l(\mathbf{x}_i).$$

This is the arithmetic mean of $u_k(\mathbf{x}_i) u_l(\mathbf{x}_i)$ and hence can again be computed by applying CP to the ‘‘observations’’ $z_i = u_k(\mathbf{x}_i) u_l(\mathbf{x}_i)$ (again, this requires each sensor to know only its own position). Since \mathbf{G} is symmetric, $\frac{L(L+1)}{2}$ (parallel) instances of CP are sufficient to obtain estimates $\hat{\mathbf{G}}_i^{(n)}$ of \mathbf{G} at each sensor. Because $\mathbf{G}^{-1} \mathbf{u}_i = I \mathbf{u}_i^\#$, estimates of $I \mathbf{u}_i^\#$ can be computed at each sensor by multiplying \mathbf{u}_i with the (possibly regularized) inverse of the CP output $\hat{\mathbf{G}}_i^{(n)}$. Since the result already incorporates the scaling factor I , the CP updates (9) and (10) can then be performed with the approximation $\mathbf{z}_i[m] \approx (\hat{\mathbf{G}}_i^{(n)})^{-1} \mathbf{u}_i y_i[m]$. We finally note that the CP-based estimation of \mathbf{G} can either be performed as a preprocessing step during the initialization phase of the WSN or in an online manner, i.e., simultaneously with the estimation of the field coefficients. In the latter case the convergence results of [4, 5] no longer apply.

4. SIMULATION RESULTS

Simulation Setup. In this section, we illustrate the performance of our CP-based field reconstruction scheme for 2-D fields via numerical simulations. The WSN consisted of sensors placed randomly following a uniform distribution over $\mathcal{A} = [0, 1] \times [0, 1]$. Communication links were established between sensors whose distance was less than $\frac{\gamma}{\sqrt{T}}$, with $\gamma > 0$ a parameter determining the connectivity of the WSN. The resulting communication graph corresponds to a random geometric graph [10].

For the subspace model, we used $L = 16$ separable basis functions (see (4)) induced either by four Legendre polynomials, four complex exponentials (Fourier basis), four Slepian sequences [11], or four Walsh functions (all appropriately scaled to the region \mathcal{A}). Moreover, we assume noise-free measurements.

Approximate orthogonalization. We first illustrate the accuracy of the approximation (11). Fig. 1 shows for the different bases the normalized Frobenius norm $\frac{1}{L} \|\frac{1}{I} \mathbf{U}^T \mathbf{U} - \mathbf{I}_L\|_F^2$, averaged over $\frac{5 \cdot 10^5}{I}$ WSN scenarios, versus the number of sensors. It is seen that as the number of sensor increases, the approximation (11) gets consistently better, with Fourier and Slepian sequences showing the most favorable behavior.

Static Fields. We next constructed a static field using a subspace model based on Legendre polynomials with randomly generated time-invariant coefficients \mathbf{c} . The field coefficients were estimated assuming that each node knows all sensor positions and hence $\mathbf{u}_i^\#$. We consider using (9), (10), i.e., the normalized mean-square error (MSE)

$$\epsilon^2[n] = \frac{1}{I} \sum_{i=1}^I \frac{\|\mathbf{c} - \hat{\mathbf{c}}_i^{(n)}\|^2}{E\{\|\mathbf{c}\|^2\}}.$$

The left part of Fig. 2 shows $\epsilon^2[n]$, which is the average of $\epsilon^2[n]$ over 100 scenarios, versus the CP parameter β for $n = 100$ and $n = 1000$ (a scenario corresponds to a realization of the field and the WSN). We considered WSN with 100, 300, and 500 sensors and chose the parameter γ to ensure identical communication range in all three cases such that connectivity increases. For fixed n , it is seen that better connectivity results in smaller MSE, provided the attenuation parameter β is decreased correspondingly in order to deal appropriately with the increasing number of loops. Furthermore, for increasing number of iterations, the minimal MSE is achieved with correspondingly higher β , well in agreement with [1].

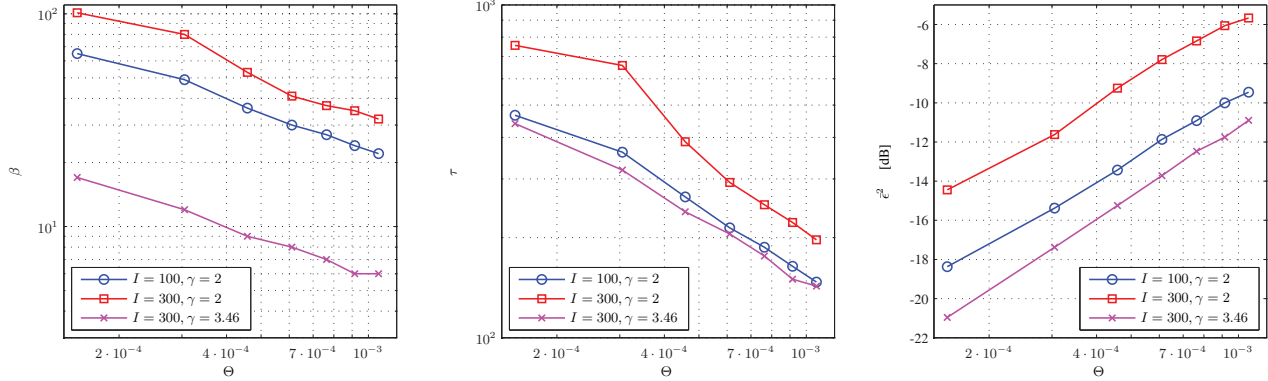


Fig. 3. Dynamic field reconstruction: optimal β (left), optimal τ (middle), and minimum MSE (right), all versus the temporal field bandwidth Θ for different WSN.

The right part of Fig. 2 illustrates the convergence behavior of the different variants of our proposed scheme by plotting the MSE versus the number of iterations. Surprisingly, the ‘preprocessing’ variant, in which $\mathbf{u}_i^\#$ is computed using 1000 CP iterations in an initialization phase, even outperforms the ‘exact’ variant in which $\mathbf{u}_i^\#$ is assumed perfectly known. The least complex ‘approximation’ variant based on (11) performs worst while the ‘online’ variant, which computes $\mathbf{u}_i^\#$ in parallel to the field coefficients, initially behaves similar to the ‘approximation’ variant but approaches the performance of the ‘exact’ variant after several hundred iterations.

Dynamic Fields. For the dynamic case, the fields were simulated using Legendre polynomials and time-varying field coefficients $\mathbf{c}[m]$ that were generated as stationary low-pass processes with cutoff frequency Θ . The field coefficients were estimated using the ‘exact’ variant of the proposed scheme with one iteration per sampling period (i.e., $n = m$). In this setup, the CP parameter β and estimation delay τ can be designed to minimize the normalized MSE between $\mathbf{c}_i[m - \tau]$ and $\hat{\mathbf{c}}_i^{(m)}[m]$ (averaged over 500 time slots and 500 scenarios). The resulting optimal parameters and minimal MSE are shown in Fig. 3 for various WSN parameters. It is seen that more rapidly varying fields require smaller β such that CP averages only locally and is thus more agile. Similarly, the estimation delay decreases with increasing Θ . However, since the averaging is more and more local with increasing cutoff frequency, the MSE increases correspondingly. This effect could be partially compensated for by increasing the number of CP iterations per time slot.

With regard to WSN topology, it is seen that large well-connected networks ($I = 300, \gamma = 3.46$) perform better than small networks with the same connectivity ($I = 100, \gamma = 2$), whereas the worst performance is incurred with large, poorly connected networks ($I = 300, \gamma = 2$).

5. CONCLUSION

The main contribution of this paper is the adaptation of the consensus propagation (CP) algorithm, originally conceived for the distributed computation of scalar averages, to a field reconstruction scenario. Building on a low-dimensional subspace model for the field, we developed a fully distributed CP-based implementation of the LS estimator of the channel coefficients, in which the sensors exchange vector messages with the neighboring nodes within their communication range. With this field reconstruction protocol, each sensor needs to know only its own position and the basis functions underlying the subspace model. Simulation results for static and dynamic

environments confirmed the usefulness of our approach. Our future work targets a convergence analysis for the dynamic case and an extension to scenarios with moving sensors.

REFERENCES

- [1] C. C. Moallemi and B. Van Roy, “Consensus propagation,” *IEEE Trans. Inf. Theory*, vol. 52, no. 11, pp. 4753–4766, Nov. 2006.
- [2] S. Boyd, A. Ghosh, B. Prabhakar, and D. Shah, “Randomized gossip algorithms,” *IEEE Trans. Inf. Theory*, vol. 52, pp. 2508–2530, June 2006.
- [3] R. Olfati-Saber, J. Fax, and R. Murray, “Consensus and cooperation in networked multi-agent systems,” *Proc. IEEE*, vol. 95, no. 1, pp. 215 – 233, Jan. 2007.
- [4] Y. Weiss and W. T. Freeman, “Correctness of belief propagation in Gaussian graphical models of arbitrary topology,” *Neural Computation*, vol. 13, no. 10, pp. 2173–2200, Oct. 2001.
- [5] J. Johnson, D. Malioutov, and A. Willsky, “Walk-sum interpretation and analysis of Gaussian belief propagation,” in *Advances in Neural Information Processing Systems 18*, Y. Weiss, B. Schölkopf, and J. Platt, Eds., pp. 579–586. MIT Press, Cambridge, MA, 2006.
- [6] C. C. Moallemi, *A Message-Passing Paradigm For Optimization*, Ph.D. thesis, Stanford University, Sept. 2007.
- [7] V. Schwarz, C. Novak, and G. Matz, “Broadcast-based dynamic consensus propagation in wireless sensor networks,” in *Proc. 43th Asilomar Conf. Signals, Systems, Computers*, Pacific Grove (CA), Nov. 2009.
- [8] O. Shental, D. Bickson, P. H. Siegel, J. K. Wolf, and D. Dolev, “Gaussian belief propagation for solving systems of linear equations: Theory and application,” *arXiv cs.IT 0810.1119v1*.
- [9] A. Ihler, J. Fisher, R. Moses, and A. Willsky, “Nonparametric belief propagation for self-localization of sensor networks,” *IEEE Journal on Selected Areas in Communications*, vol. 23, no. 4, pp. 809 – 819, April 2005.
- [10] Mathew Penrose, *Random Geometric Graphs*, Oxford University Press, 2003.
- [11] D. Slepian, “Prolate spheroidal wave functions, Fourier analysis, and uncertainty—V: The discrete case,” *Bell System Technical Journal*, vol. 57, no. 5, pp. 1371–1430, 1978.